Light scattering by hexagonal water ice crystals

D.N. Romashov

Institute of Atmospheric Optics,
Siberian Branch of the Russian Academy of Sciences, Tomsk

Received December 22, 2000

The beam splitting method (BSM), used in calculation of light-scattering polarization characteristics for randomly oriented hexagonal water ice crystals, is described. The method is compared with the ray tracing method. The scattering phase matrices (SPM) of monodisperse ensembles of randomly oriented hexagonal water ice crystals, calculated by the BSM, are presented and analyzed. Their dependence on size and shape of hexagonal water ice crystals for the incident radiation of 0.55 and 0.67 μm wavelengths is studied.

1. Beam splitting method

The majority of calculations on the optical characteristics of light scattering by hexagonal water ice crystals available have been carried out in the geometric optics approximation[1–5] based on the geometric and physical analysis of the ray propagation inside a polyhedron according to the general Snellius and Fresnel laws (taking into account absorption[6]). The principal disadvantage of this approximation is that it assumes the contribution from the rays going out of the crystal to the scattered radiation in the far zone to occur only in the direction the rays go out from the crystals. Many researchers who use this approximation limit themselves by calculating only the scattering phase function and the degree of polarization of radiation scattered by the ensembles of randomly oriented hexagonal crystals.

Most comprehensively the geometric optics approximation has been realized in calculations of all components of the scattering phase matrix in the ray tracing method (RTM).[1,2] The calculated results[1] on the elements of scattering phase matrix P_{33} and P_{44} of ensembles of randomly oriented ice crystals differ from analogous results calculated for spheroids[7] and the data of measurements of artificial ice crystals.[8] So RTM was essentially modernized in Ref. 2. New weighting coefficients for the reflected and refracted rays are introduced in the modernized RTM. Intensities of diffracted rays, externally reflected rays, the rays that experienced several internal reflections, and the rays refracted outside are summed. Interference is taken into account only for the backscatter for two mutual rays. One can analytically write it as follows:

$$\mathbf{G}^{\mathrm{S}} = \mathbf{G}^{\mathrm{D}} + \sum_{rn} \mathbf{G}^{\mathrm{RT}}_{rn},$$

where $\mathbf{G}^{\mathrm{S}}$ is the scattering phase matrix of the crystal, $\mathbf{G}^{\mathrm{D}}$ is the contribution due to the wave diffraction on the crystal to the scattering phase matrix, $\mathbf{G}^{\mathrm{RT}}_{rn}$ is the contribution from the externally reflected ($n = 1$) or going out of the crystal rays, rn is the number of the ray that underwent n interactions with a crystal side.

The ray scattering phase matrix $\mathbf{G}^{\mathrm{RT}}_{rn}$ is calculated by means of the matrix of transformation of the ray amplitudes (RA) $\mathbf{S}^{\mathrm{RT}}_{rn}$ by formulas presented in Ref. 9. The formula for RA in the ray tracing method[2] has the form:

$$\mathbf{S}^{\mathrm{RT}}_{rn}(\mathbf{e}^{S}) = \mathbf{A}^{\mathrm{RT}}_{rn}\, q_{rn}(\mathbf{e}^{\mathrm{S}}) \exp(ikNd_{rn}); \qquad (1)$$

$$q_{rn}(\mathbf{e}^{\mathrm{S}}) = \delta(1 - \mathbf{e}^{\mathrm{S}}\,\mathbf{e}^{rn})\, w_{rn}; \qquad (2)$$

$$w^2_{r1} = \cos\theta^{\mathrm{I}}_{r1} / \sin\theta^{\mathrm{S}};$$

$$w^2_{rn} = \frac{\cos\theta^{\mathrm{T}}_{r1}}{\cos\theta^{\mathrm{I}}_{r1}} \frac{\cos\theta^{\mathrm{T}}_{rn}}{\cos\theta^{\mathrm{I}}_{rn}} \frac{\cos\theta^{\mathrm{I}}_{r1}}{\sin\theta^{\mathrm{S}}}, \quad n \geq 2,$$

where $\mathbf{A}^{\mathrm{RT}}_{rn}$ is the matrix of transformation of amplitudes of the ray electric field at reflection and refraction at the crystal surfaces, $\mathbf{e}^{\mathrm{S}}$ is the unit vector along the direction of scattering, $\mathbf{e}^{rn}$ is the unit vector along the direction of the ray going out of the crystal, $\delta(x)$ is the Dirac delta-function, i is imaginary unit, k is the wave number, N is the complex refractive index, d_{rn} is the length of the geometric path of the ray inside the crystal, w_{rn} are the weighting coefficients of the electric field for the rays at slant incidence on the crystal side, θ^{I}_{r1} and θ^{T}_{r1}, respectively, are the angle of incidence and the angle of refraction of the ray at the first interaction with the crystal, θ^{I}_{rn} and θ^{T}_{rn}, respectively, are the angle of incidence and the angle of refraction of the ray going out of the crystal, θ^{S} is the scattering angle.

The use of the geometric optics approximation is justified when studying the ray trajectories inside the crystals the size of which is much greater than the wavelength, as well as when calculating the electric fields formed by them in the near zone. When recalculating the electric fields from near zone to the far zone, the geometric optics approximation is very rough. In particular, it results in an uncertainty of the

0235-6880/01/02 102-09 $02.00

RTM calculation of the weighting coefficients for the scattering angles $\theta^S = 0$ or π. Authors of Ref. 2 avoid this uncertainty by assuming that in this cases $\sin\theta^S = \sin(\pi/360)$. The conclusion following from the RTM calculations, that the scattering phase matrix $\mathbf{G}^{RT}$ for an arbitrary transparent hexagonal ice crystal normalized to the cross section depends not on the crystal size but on the ratio L/a (L is the crystal axis length, a is the hexagonal side edge length) is not physically justified for a wide size spectrum of real atmospheric crystals. This assertion is correct only for very large crystals, as it will be shown below.

The disadvantages of RTM are overcome in the beam splitting method (BSM) proposed for the first time in Ref. 10 and modernized in Ref. 11. In contrast to RTM, the BSM deals not with the rays but with the bunches of rays, or beams. Beam is understood as a set of elementary rays, which have undergone the same interactions with the same sides of a polyhedron. The cross section of the reflected beam at the first interaction of a plane wave with any side is the projection of this side onto the plane perpendicular to the reflected beam. One can advance analogous arguments for the beam refracted into a crystal after the first interaction. The beam refracted into the crystal can be incident on several sides, i.e., the beam is divided on tops and edges. It is clear that the cross sections of the beams going out of the polyhedron have the polygonal shape and their area decreases after each inner reflection and refraction outside (except for the cases when the beam has completely fitted one side).

Thus, the process of tracing the beam formation in the BSM (as that of the ray trajectories in the RTM) and calculations of the beam fields in near zone are carried out by use of the geometric optics approximation. The contribution of a beam to the scattered field in the far zone is estimated in the approximation of Fraunhofer diffraction on the aperture coinciding with the beam cross section. The algorithm for calculation of the plane wave diffraction on the aperture of an arbitrary polygonal shape is presented in Ref. 11.

The scattering phase matrix (SPM) is represented in BSM,[11] the same as in RTM[2] in the form of the sum of diffracted and reflected-refracted scattering phase matrices:

$$\mathbf{G}^S = \mathbf{G}^D + \mathbf{G}^{RT},$$

Depending on the input parameters (roughness of the crystal sides, crystal size, and wavelength of the incident radiation), the problem of determining the SPM of a crystal $\mathbf{G}^{RT}_{rn}$ is solved in two ways:

1) without the account for interference between the beams $\mathbf{G}^{RT} = \sum_{bn} \mathbf{G}^{RT}_{bn}$, where $\mathbf{G}^{RT}_{bn}$ is the scattering phase matrix of the beam that underwent n interactions with the sides, which is calculated using RA of the beam $\mathbf{S}^{RT}_{bn}$; bn is the number of the beam that underwent n interactions with the sides.

2) taking into account the interference between the beams: SPM of an arbitrary crystal $\mathbf{G}^{RT}$ is determined using the total RA $\mathbf{S}^{RT} = \sum_{bn} \mathbf{S}^{RT}_{bn}$.

In the backscatter case the interference between the mutual beams should be always taken into account.

For a convenience in comparing the BSM with the RTM let us restrict ourselves to consideration of non-absorbing crystals. In the case of absorbing crystals the formulas for RA have more cumbersome and inconvenient form (as compared with formulas (1)–(2)), because the field amplitude in the beam cross section plane is different, and one should use the adjusted refractive index for calculation of the elementary beam phase shift between two successive interactions inside the crystal.[6]

The formula for RA of the beam going out (or externally reflected) of the non-absorbing crystal undergone n interactions with the crystal sides has the following form in the BSM[11]:

$$\mathbf{S}^{RT}_{bn}(\mathbf{e}^S) = \mathbf{A}^{RT}_{bn}\, q_{bn}(\mathbf{e}^S) \exp(ikNd_{bn}), \qquad (3)$$

$$q_{bn}(\mathbf{e}^S) = \frac{k^2}{4\pi} \iint_{G_{bn}} \exp(-ik\mathbf{e}^S \cdot \mathbf{r})\, d^2\mathbf{r}\,, \qquad (4)$$

where $\mathbf{A}^{RT}_{bn}$ is the matrix of transformation of the amplitudes of the electric field components on the crystal sides.[12] The geometric phase shift of the beam d_{bn} is considered as the mean maximum of all geometric shifts of elementary rays belonging to same beam at the point of their going out of the side relative to the crystal center; G_{bn} is the beam cross section, $\mathbf{r}$ is the radius-vector of a point in the beam cross section.

Obviously, at the same sequence of interactions of rn-ray in Eq. (1) and bn-beam in Eq. (3) with the sides $\mathbf{A}^{RT}_{rn} = \mathbf{A}^{RT}_{bn}$. So the form of the factors $q_{rn}(\mathbf{e}^S)$ in Eq. (1) and $q_{bn}(\mathbf{e}^S)$ in Eq. (3) shows the principal difference between the RTM and BSM methods.

It is seen from formula (4) that, as the beam cross section size G_{bn} increases, the greater portion of its intensity is concentrated near the direction the beam goes out of the crystal, and vice versa. As the geometrical analysis of the processes of beam formation on an arbitrary crystal shows, the beam size decreases as the number of interactions between sides increases, and their quantity increases inversely proportional to their cross sections. Besides, the beams, one of the size of which is quite small, at the incidence angles close to $\pi/2$, are formed even in the cases of external reflection from big sides. On the other hand, as the multiplicity of interactions n increases, the absolute values of the elements of the matrix $\mathbf{A}^{RT}_{bn}$ tend to zero. BSM provides for simultaneously take into account the effect of all the above-mentioned factors, in contrast to RTM, in which all rays are equivalent in their contribution to the total intensity of scattering.

The method of integral equation of geometric optics (GOM2) was proposed in Ref. 12 for calculating

the light scattering characteristics of hexagonal water ice crystals. Comparison of the BSM with GOM2 was presented in Ref. 11, and showed good agreement with the calculated results on the SPM. Unfortunately, calculations of the elements of the scattering phase matrix presented in Ref. 12 were made only for small size ($ka = kL \le 200$), and comparison of the results obtained by means of GOM2 and BSM was performed only for two elements of SPM: P_{11} and $-P_{12}/P_{11}$. As it will be shown below, large differences in results calculated by use of the RTM and BSM are observed for three elements of SPM: P_{22}/P_{11}, P_{33}/P_{11}, and P_{44}/P_{11}.

2. Scattering phase matrices of monodisperse ensembles of randomly oriented hexagonal ice crystals. Effects of size and shape

The majority of scattering phase matrices of ensembles of randomly oriented hexagonal ice crystals presented in this paper were calculated by means of the BSM without the account of interference between the beams. The cases when interference between the beams was taken into account are noted especially.

Let us first define the principal input parameters of the problem of light scattering by a hexagonal ice crystal. Let us represent the crystal size by its length along its symmetry axis L and the radius of circle a circumscribed around the hexagonal basis. The value $d = 2a$ is called the crystal diameter. Let the hexagonal crystal shape be characterized by the ratio d/L. Such bodies at $L > d$ are usually called hexagonal columns, and at $L < d$ – hexagonal plates.

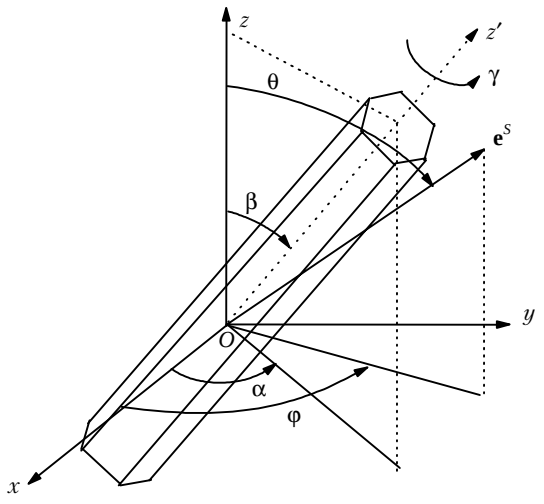

Fig. 1. Geometry of scattering on an arbitrarily oriented hexagonal crystal.

Let us describe the geometry of scattering of radiation on an arbitrarily oriented crystal. Let us define the coordinate system $Oxyz$ (Fig. 1) related to the incident radiation as follows: the direction of the axis Oz coincides with the direction of the incident radiation propagation. Let the coordinate system $Ox'y'z'$ be obtained from $Oxyz$ by turning to three Euler angles α, β, and γ and be related to the crystal as follows: the point O is at the crystal center, the axis Oz' is the axis of symmetry of the crystal, the axis Ox' is perpendicular to one of the quadrangular sides.

Thus, β is the angle between the direction of the incident radiation and the crystal axis, α is the angle between the plane xOz and the plane formed by the Oz axis and the crystal axis, γ is the angle of turning around the crystal axis. The direction of scattering is set by the polar angle θ and the azimuth angle φ in the coordinate system $Oxyz$.

As all the scattering planes for isotropic ensembles are equivalent, to determine $\mathbf{P}$ (SPM of the monodisperse ensemble of randomly oriented hexagonal crystals), it is necessary to average over all orientations in the 3D space at a fixed arbitrary scattering plane (for example, $\varphi = 0$). But as averaging over the angle α is equivalent to averaging over the scattering planes φ with the fixed value of the angle α, the averaged over two angles β and γ phase matrix of scattering to the total solid angle of crystals randomly oriented in the plane xOz was first calculated in this paper:

$$\mathbf{F}(\theta, \varphi) = \frac{6}{\pi} \int_0^{\pi/2} \int_0^{\pi/6} \mathbf{G}(\theta, \varphi, \beta, \gamma) \sin\beta \, d\beta \, d\gamma,$$

where $\mathbf{G}(\theta, \varphi, \beta, \gamma)$ is the SPM of a crystal oriented at the angles $\alpha = 0$, β, and γ. Then the SPM of the ensemble of randomly oriented crystals was calculated by means of averaging of the SPM $\mathbf{F}(\theta, \varphi)$ over the scattering planes set by the angle φ:

$$\mathbf{P}(\theta) = \frac{1}{2\pi} \int_0^{2\pi} \mathbf{F}(\theta, \varphi) \, d\varphi.$$

The SPM element P_{11} is normalized in all calculations presented in this paper as follows:

$$\int_0^{\pi} \mathbf{P}(\theta) \sin\theta \, d\theta = 1.$$

When calculating $\mathbf{P}(\theta)$, averaging over the orientation angles was performed on the following grid:

$$\beta_j = 0.5° \, j; \quad j = 0, 1, \ldots, 180;$$

$$\gamma_l = 0.5° \, l; \quad l = 0, 1, \ldots, 60.$$

The grid of the scattering angles was set as follows:

$$\varphi_m = 1° \, m; \quad m = 0, 1, \ldots, 359;$$

$$\theta_s = 0.1° \, s; \quad s = 0, 1, \ldots, 9,$$

$$\theta_s = 1° \, (s - 9); \quad s = 10, 11, \ldots, 189.$$

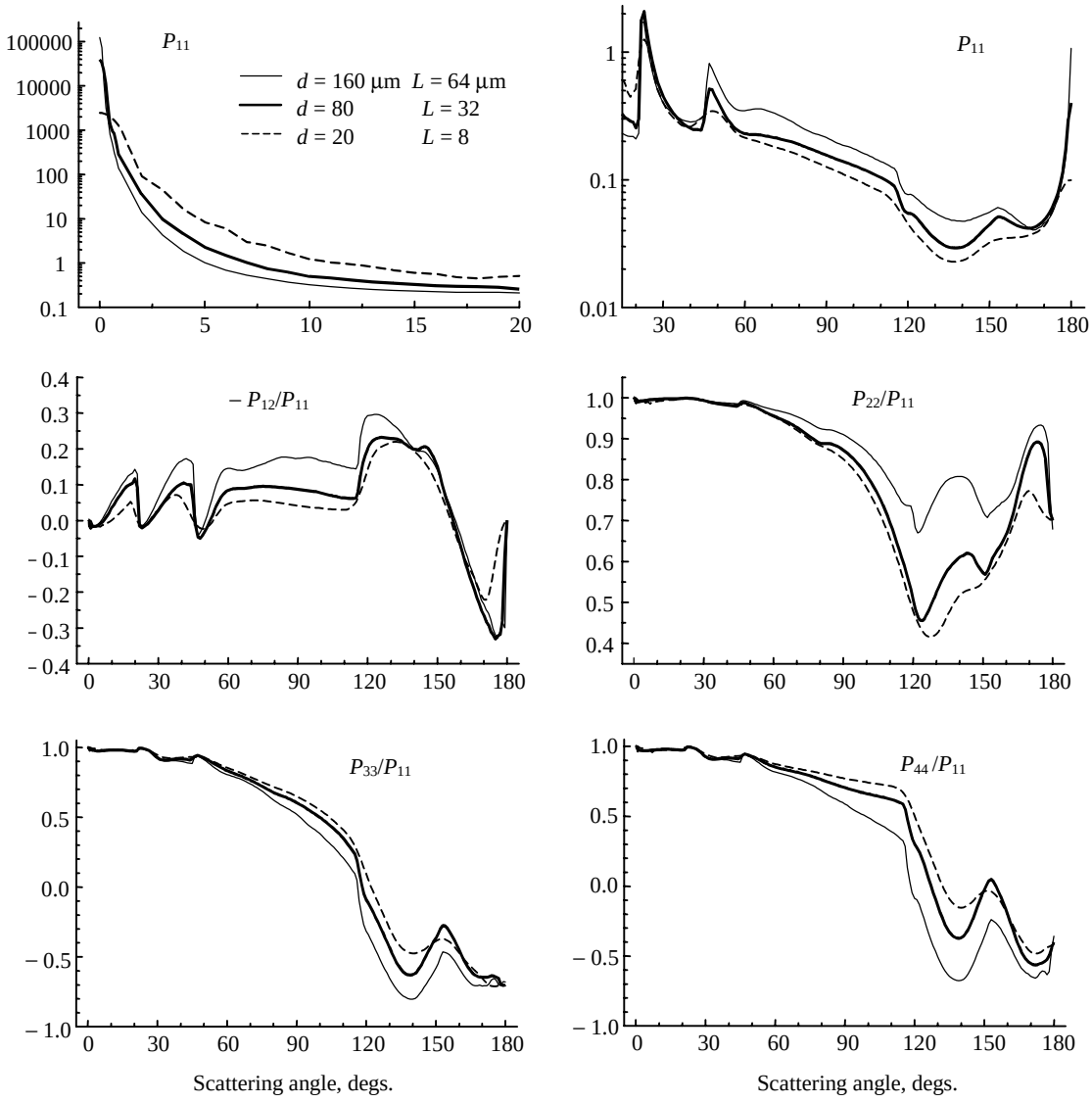

Fig. 2. Elements of the scattering phase matrices of monodisperse ensembles of randomly oriented hexagonal ice plates with the same d/L ratio.

Five elements of the normalized SPM are shown in Fig. 2 for three monodisperse ensembles of randomly oriented hexagonal ice plates with the same value of the ratio $L/d = 2/5$ for the wavelength of the incident radiation $\lambda = 0.55$ μm and the refractive index $N = 1.311$. It is well seen in the behavior of the curves in Fig. 2 that, as the crystal size increases, the dependence of the elements of normalized SPM on the scattering angle θ has different shape. Let us discuss the most essential differences:

– the increase of the values of the scattering phase function $P_{11}(\theta)$ with the increase of the plate size for the scattering angles $\theta = 0$, 22°, and $\theta \geq 46°$, the most significant increase is observed at $\theta = 0$, 180, and 46°;

– the decrease of the values of the scattering phase function $P_{11}(\theta)$ with the increase of the plate size for the scattering angles $0° < \theta < 20°$;

– the increase of the values of the degree of polarization $-P_{12}(\theta)/P_{11}(\theta)$ with the increase of the plate size for the scattering angles $0° < \theta < 140°$ (analogous tendency is observed in calculated data on this value presented in Ref. 13);

– the increase of the values $P_{22}(\theta)/P_{11}(\theta)$ with the increase of the plate size for the scattering angles $60° < \theta < 170°$;

– the decrease of the values $P_{33}(\theta)/P_{11}(\theta)$ and $P_{44}(\theta)/P_{11}(\theta)$ with the increase of the plate size for the scattering angles $60° < \theta < 150°$;

– the values $P_{22}(180°)/P_{11}(180°)$, $P_{33}(180°)/P_{11}(180°)$ and $P_{44}(180°)/P_{11}(180°)$ practically do not depend on the plate size.

Let us note that the values $P_{34}(\theta)/P_{11}(\theta)$, not shown in Fig. 2, very weakly depend on the plate size for all scattering angles θ.

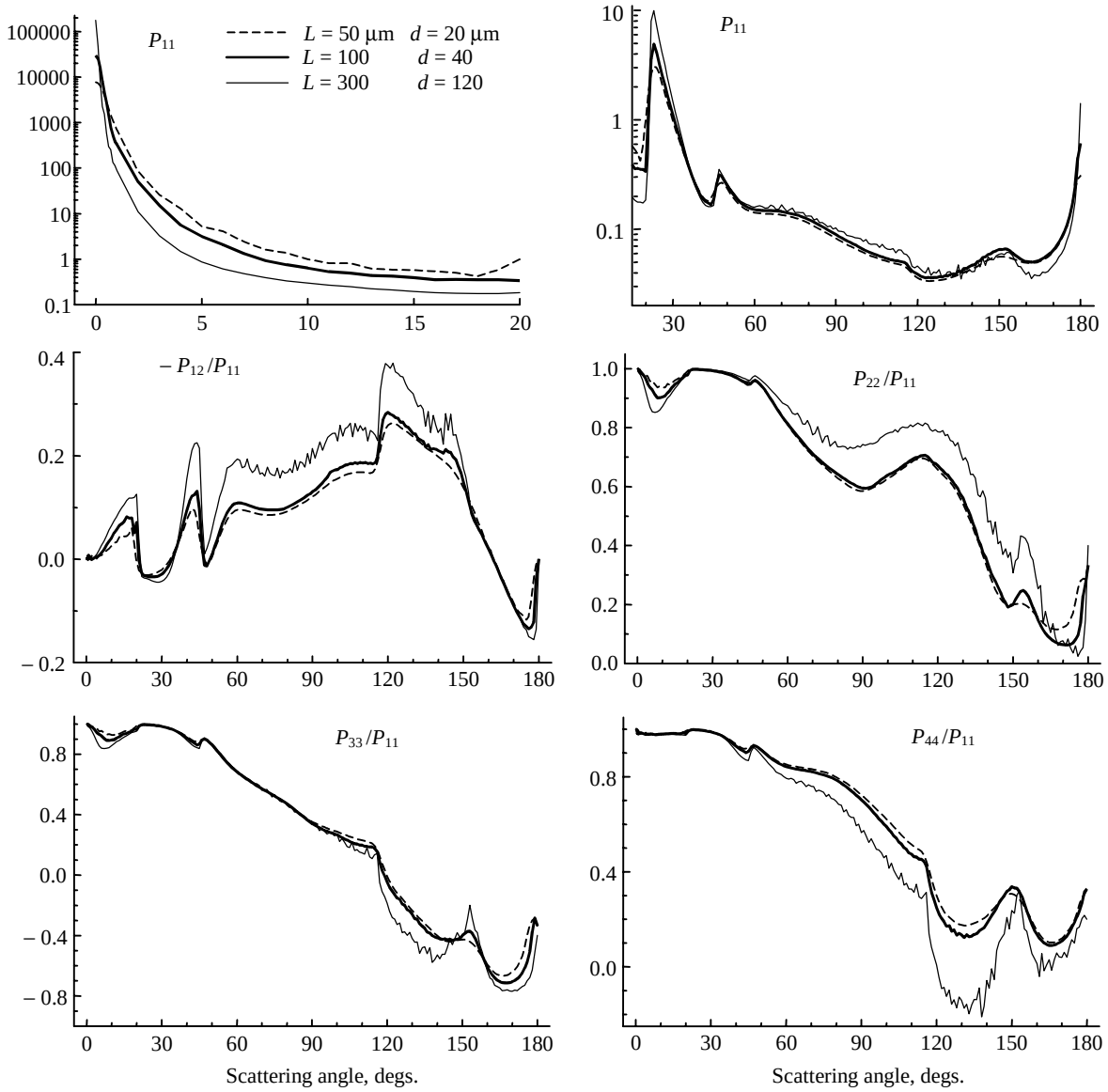

Fig. 3. Elements of the scattering phase matrices of monodisperse ensembles of randomly oriented hexagonal ice columns with the same d/L ratio.

Six elements of the normalized scattering phase matrix of randomly oriented hexagonal ice plates of the size $L = 8$ μm, $d = 20$ μm at $\lambda = 0.6328$ μm and $N = 1.311$ are presented in Ref. 2, and four elements of normalized SPM of randomly oriented hexagonal ice plates of the size $L = 32$ μm, $2a = 80$ μm at $\lambda = 0.55$ μm and $N = 1.311 + 9.11i10^{-9}$ are presented in Ref. 3. As would be expected, the dependences of four elements of the SPM presented in Ref. 2 and Ref. 3 $P_{22}(\theta)/P_{11}(\theta)$, $P_{33}(\theta)/P_{11}(\theta)$, $P_{44}(\theta)/P_{11}(\theta)$, and $P_{34}(\theta)/P_{11}(\theta)$ coincide and differ from the analogous shown in Fig. 2. In the subsequent comparison of the results let us mark the values calculated by means of RTM with a superscript r, and by BSM with b.

The greatest differences are observed between calculated elements $P_{11}(\theta)$, $P_{22}(\theta)/P_{11}(\theta)$, $P_{33}(\theta)/P_{11}(\theta)$, and $P_{44}(\theta)/P_{11}(\theta)$ presented in Ref. 2 and in Fig. 2 for small plates with $L = 8$ μm and $d = 20$ μm. These differences are the following:

- the values $P_{11}^{r}(\theta) < P_{11}^{b}(\theta)$ for $1 < \theta < 21°$;
- $P_{11}^{r}(\theta) > P_{11}^{b}(\theta)$ for $21 < \theta < 180°$;
- $P_{11}^{r}(180°) \gg P_{11}^{b}(180°)$;
- $P_{11}^{r}(22°) \gg P_{11}^{b}(22°)$;
- $P_{11}^{r}(46°) \gg P_{11}^{b}(46°)$;
- $P_{22}^{r}(\theta)/P_{11}^{r}(\theta) < P_{22}^{b}(\theta)/P_{11}^{b}(\theta)$ for $120 < \theta \le 180°$;
- $P_{33}^{r}(\theta)/P_{11}^{r}(\theta) > P_{33}^{b}(\theta)/P_{11}^{b}(\theta)$ for $140 < \theta \le 180°$;
- $P_{44}^{r}(\theta)/P_{11}^{r}(\theta) > P_{44}^{b}(\theta)/P_{11}^{b}(\theta)$ for $140 < \theta \le 180°$.

Five elements of the normalized SPM for three monodisperse ensembles of randomly oriented hexagonal ice columns with the same value of the ratio $L/d = 5/2$ at $\lambda = 0.55$ μm and the refractive index $N = 1.311$ are shown in Fig. 3. It is seen in the behavior of the curves presented in Fig. 3 that the same

tendencies are observed in the behavior of the normalized SPM with the increase of the crystal size, as it was observed for the plates in Fig. 2. Let us note that, in contrast to plates, more significant increase of $P_{11}(\theta)$ is observed as the crystal size increases and at $\theta = 0$, $\theta = 180°$, and $\theta = 22°$ (not at $\theta = 46°$ as it was for plates).

Comparison of the elements of the SPM of hexagonal ice columns of the size $L = 300$ μm and $a = 60$ μm shown in Fig. 3 with analogous elements of the SPM of hexagonal ice columns of the same size presented in Ref. 2 shows that their angular behaviors are very similar. However, there are essential differences:

– the values $P_{11}^{r}(46°) > P_{11}^{b}(46°)$;

– $P_{11}^{r}(150°) > P_{11}^{b}(150°)$;

– peak of $P_{44}^{b}(\theta)$ near $\theta = 150°$ is more narrow than the peak of $P_{44}^{r}(\theta)$;

– the presence of the well pronounced peak of $P_{33}^{b}(\theta)$ near $\theta = 150°$ and its absence for $P_{33}^{r}(\theta)$.

To investigate the effect of shape, the calculations were performed for the crystals with different values of the ratio $L/d = 1/4$, 1, and 4, but with the same value of the equivalent radius. The equivalent radius of a non-spherical particle is considered to be the value equal to the ratio of three volumes of the particle to the area of its surface. The elements of the SPM of three ensembles of randomly oriented hexagonal ice crystals with the same value of the equivalent radius 44.3 μm but with different values of the ratio L/d at the wavelength of the incident radiation $\lambda = 0.67$ μm and the refractive index $N = 1.3076$ are shown in Fig. 4. It is seen from the curves shown in Fig. 4 that the shape of the hexagonal crystal essentially affects both the distribution of the scattered radiation over the total solid angle and the state of polarization of the radiation scattered along any direction.

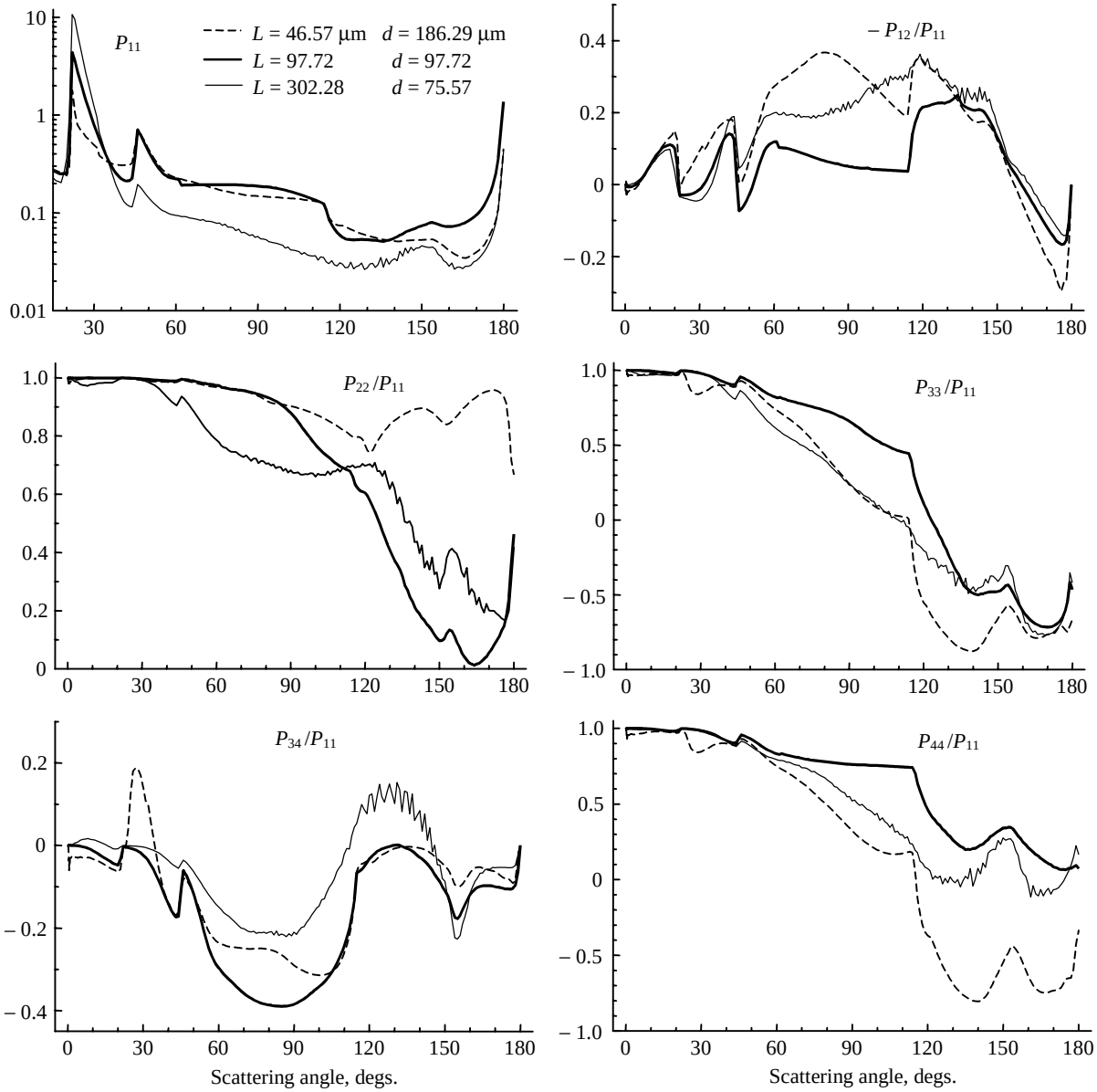

Fig. 4. Elements of the scattering phase matrices of monodisperse ensembles of randomly oriented hexagonal ice columns of the same equivalent radius.

The calculated results on the SPM of three ensembles of randomly oriented hexagonal ice plates, the thickness of which is related to the diameter d by the empirical relationship[14]

$$L = 0.6\, d^{0.8}$$

are shown in Fig. 5. The data shown in Fig. 5 demonstrate the joint effect of the shape and the size on the SPM of the randomly oriented hexagonal ice plates, because the value of the ratio d/L increases as the plate diameter increases.

The elements of the SPM of the same ensembles of crystal particles as in Fig. 5 calculated by means of BSM taking into account the interference between the beams are shown in Fig. 6. Comparing the behavior of analogous elements of SPM in Fig. 5 and Fig. 6, one can conclude that the account for the interference between the beams essentially affects the calculated results for large plates (d = 200 μm), insignificantly for intermediate (d = 100 μm) and practically does not affect those for small plates (d = 30 μm).

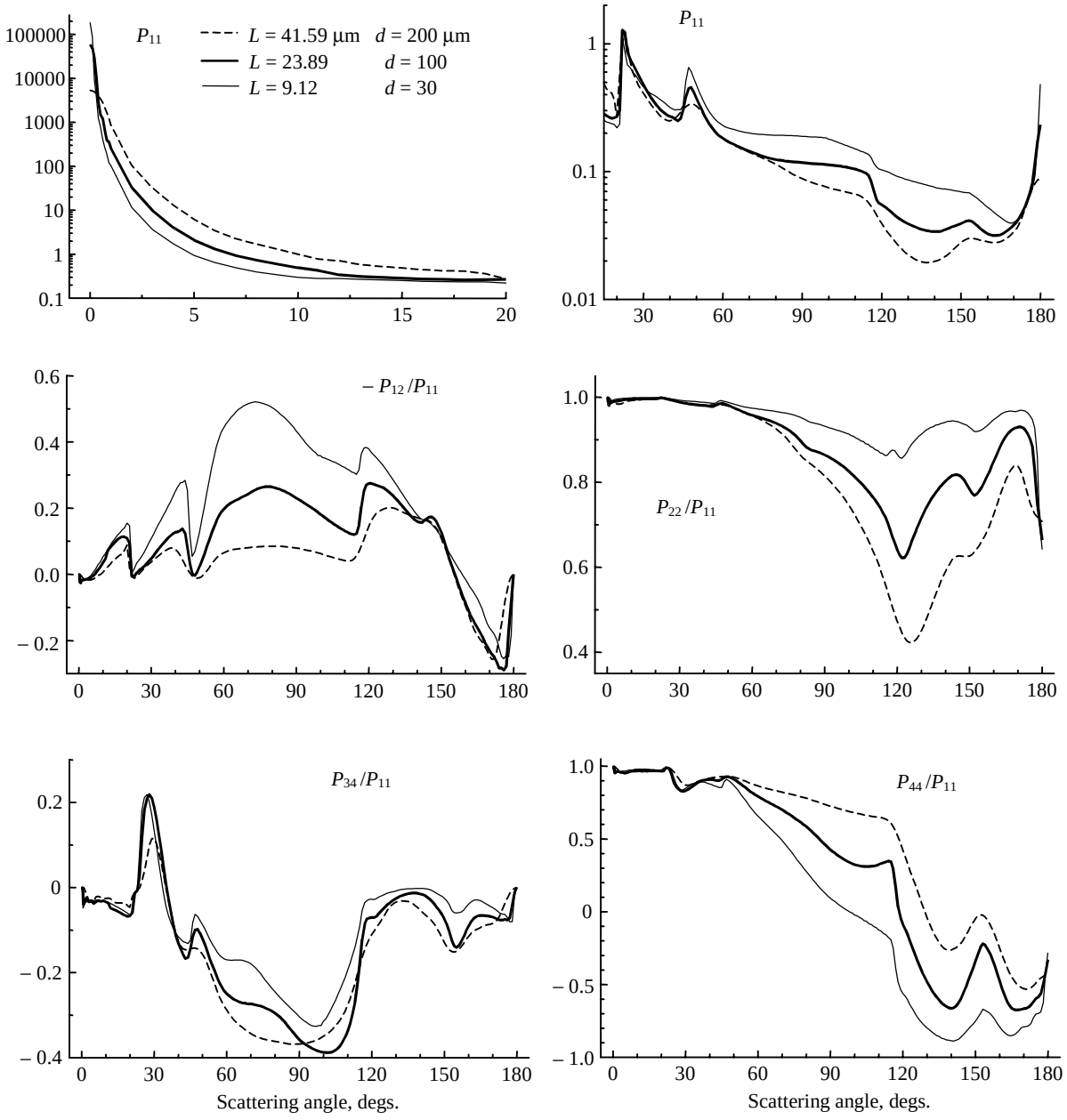

Fig. 5. Elements of the scattering phase matrices of monodisperse ensembles of randomly oriented hexagonal ice plates calculated by the BSM without the account of interference between the beams.

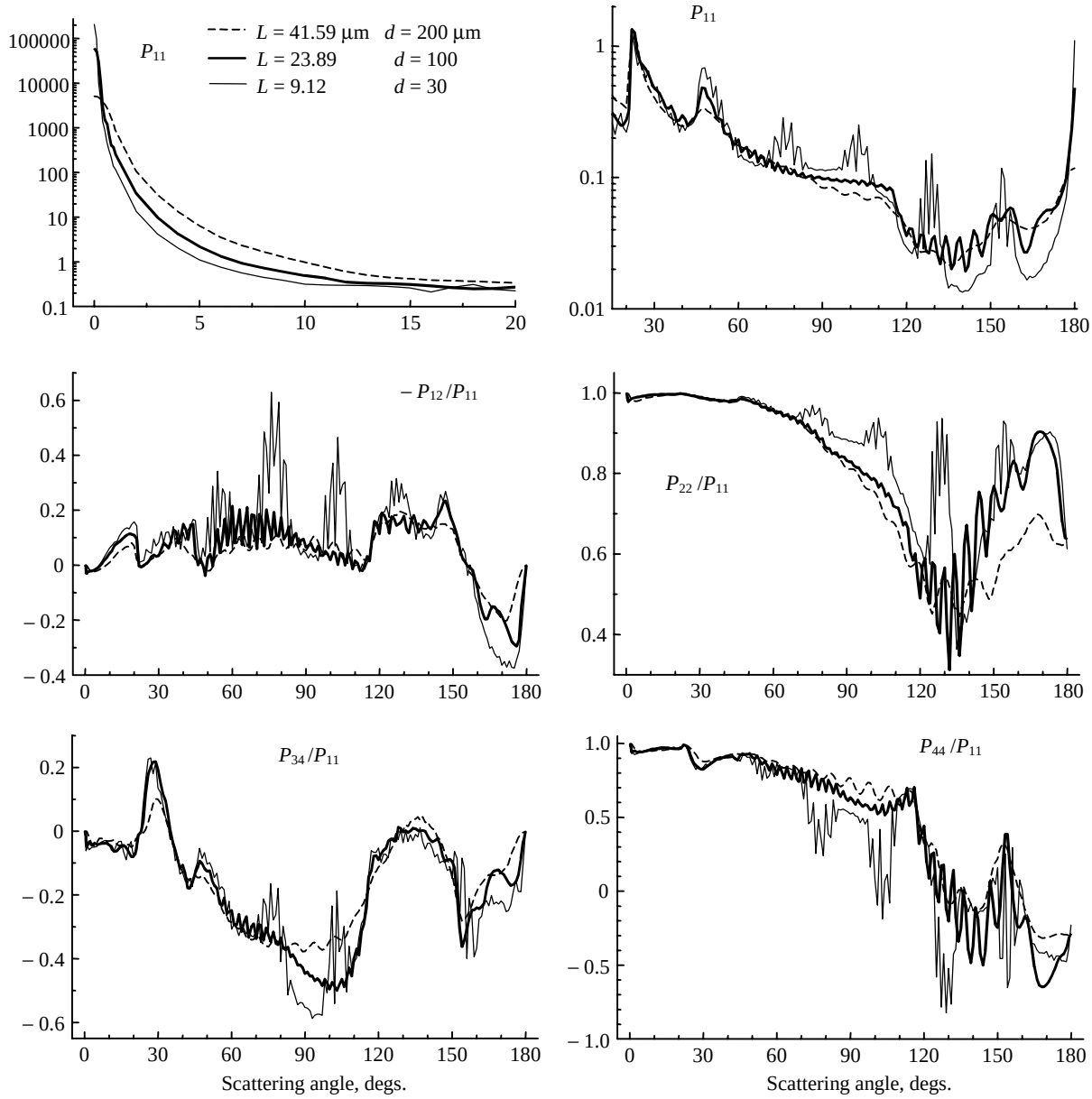

Fig. 6. Elements of the scattering phase matrices of the same ensembles of ice plates as shown in Fig. 5, but calculated by the BSM that takes into account the interference between the beams.

Thus, the aforementioned analysis shows that BSM, different from RTM, is more sensitive to the microstructure of crystals because of taking into account the diffraction of the beam fields in far zone and has not uncertainties at all scattering angles. The behavior of the elements $P_{22}(\theta)/P_{11}(\theta)$, $P_{33}(\theta)/P_{11}(\theta)$, and $P_{44}(\theta)/P_{11}(\theta)$ calculated by use of the BSM is in a better agreement with the behavior of analogous experimentally measured elements for artificial crystals[8] than the behavior of these elements calculated by means of RTM. It is better pronounced as the absence of high and wide peak of the elements $P_{33}(\theta)/P_{11}(\theta)$ and $P_{44}(\theta)/P_{11}(\theta)$ calculated by means of BSM near $\theta = 150°$ and its presence in analogous elements calculated by means of RTM.

Besides, BSM, different from RTM and other methods (GOM2, T-matrix method[15]), requires much smaller computer resources. All calculations presented in this paper were carried out on a Pentium II computer with a 300-MHz CPU.

Acknowledgments

The work was supported in part by Russian Ministry of Sciences, project "Lidar" (No. 06–21).

References

1. Q. Cai and K.N. Liou, Appl. Opt. **21**, No. 19, 3569–3580 (1982).
2. Y. Takano and K. Jeyaweera, Appl. Opt. **24**, No. 19, 3254–3263 (1985).

3. Y. Takano and K.N. Liou, Appl. Opt. **46**, No. 1, 3–19 (1989).
4. P. Wendling, R. Wendling, and H.K. Weickmann, Appl. Opt. **18**, 2663–2671 (1979).
5. K.D. Rockwitz, Appl. Opt. **28**, 4103–4110 (1989).
6. P. Yang and K.N. Liou, J. Opt. Soc. Am. A. **13**, No. 10, 2072–2085 (1996).
7. S. Asano and M. Sato, Appl. Opt. **19**, No. 6, 962–974 (1980).
8. V.P. Dugin and S.O. Mirumyants, Izv. Acad. Sci. USSR, Atmos. Oceanic. Phys. **12**, 988–991 (1976).
9. C.F. Bohren and D.R. Huffman, *Absorption and Scattering of Light by Small Particles* (Wiley, New York, 1983).
10. A.A. Popov, *Scattering of a plane electromagnetic wave on a semi-transparent convex polyhedron of arbitrary shape*, Izv. Vyssh. Uchebn. Zaved. Ser. Fizika, VINITI, No. 8006, Tomsk (1984), 56 pp.
11. D.N. Romashov, Atmos. Oceanic Opt. **12**, No. 5, 376–384 (1999).
12. P. Yang and K.N. Liou, Appl. Opt. **35**, No. 33, 6568–6584 (1996).
13. K. Muinonen. Appl. Opt. **28**, No. 15, 3044–3050 (1989).
14. A. Petrushin. Proc. SPIE **3583**, 147–154 (1998).
15. D.J. Wielaard, M.I. Mishchenko, A. Macke, and B.E. Carlson, Appl. Opt. **36**, No. 18, 4305–4313 (1997).